ELSEVIER

International Journal of Mass Spectrometry 223–224 (2003) 427–446

International Journal of Mass Spectrometry

www.elsevier.com/locate/ijms

# Negative-ion CIMS: analysis of volatile leaf wound compounds including HCN

Thomas G. Custer*, Shuji Kato, Ray Fall, Veronica M. Bierbaum

*Department of Chemistry and Biochemistry, University of Colorado, Boulder, CO 80309-0215, USA*

Received 22 January 2002; accepted 24 May 2002

We dedicate this paper to the memory of Professor Werner Lindinger, a remarkable physicist and dear friend, who pursued both life and science with incomparable vigor and enjoyment.

**Abstract**

Chemical-ionization mass spectrometry (CIMS) using flow-reactor mass spectrometers has flourished as a sensitive, on-line method of analyzing trace volatile organic compounds (VOCs) in air. In this work, the $OH^-$ anion is explored as the ionizing reagent in a flowing-afterglow selected ion flow tube (FA-SIFT) instrument for its utility in detecting VOCs and HCN released by cut and wounded plant material. Reaction rate coefficients and products for reactions between $OH^-$ anion and 17 plant VOCs and some structural isomers are reported. These results are also compared to reactions between $H_3O^+$ and these same VOCs. Fragmentation products from collision-induced dissociation (CID) of the $[M-1]^-$ anion of each species are also given to aid in ion identification. H/D exchange was successfully used to distinguish ionized aldehyde/ketone products that are structural isomers for two different isomeric aldehyde/ketone pairs. Simultaneous emissions of acetone, butanone, and HCN were observed from several plants and the emissions of acetone and butanone were confirmed from one plant using H/D exchange. The utility of this technique as a screening tool for cyanogenesis in plants is discussed. (Int J Mass Spectrom 223–224 (2003) 427–446)


*Keywords:* Negative-ion chemical-ionization; Hydroxide anion; Selected ion flow tube; Volatile organic compounds; Cyanogenesis

## 1. Introduction

Chemical-ionization mass spectrometry (CIMS), discussed in detail by Harrison [1], is an effective tool for analysis of complex mixtures of organic compounds. This technique allows selective ionization of analyte molecules and produces a minimal number of product ions compared to higher energy ionization methods such as electron ionization. Ionic products of chemical-ionization can be rapidly mass selected and detected with excellent sensitivity. A variety of chemical-ionization reagents have been used in a number of different CIMS instruments. These ions provide a convenient ion-chemistry-toolbox with which to selectively and efficiently ionize a wide variety of molecules. Some of the more commonly used anionic reagents are described by Budzikiewicz [2]. Recollections on the development of chemical-ionization including mention of several cationic reagents are given by Munson [3].

Flow-reactor mass spectrometers (such as the flowing afterglow, selected ion flow tube, and flow-drift tube) have long been used to study ion/molecule reactions that are the foundation of chemical-ionization

* Corresponding author. E-mail: thomas.custer@colorado.edu

1387-3806/02/$ – see front matter 
*PII* S1387-3806(02)00930-2

processes. A thorough description of developments in such flow-reactor techniques can be found in Graul and Squires [4]. More recently, these instruments have been adopted for on-line chemical-ionization of trace volatile organic compounds (VOCs) in air and can be found in a variety of incarnations. A few examples of these specialized air-monitoring instruments are given by Lindinger et al. [5], Smith and Spanel [6], and de Gouw et al. [7]. These studies and many others have repeatedly demonstrated excellent sensitivity and time resolution for monitoring VOCs in air for a wide variety of applications. They are particularly useful because under well-defined conditions and when individual rate coefficients are known, VOC concentrations can be calculated from measured peak height, flow-rate, and pressure data using simple equations derived from fundamental ion/molecule reaction kinetics. With this simple model, there is no need for prior calibration unless unusually high measurement accuracy is desired.

The arsenal of ion chemistry methods for flow-reactor mass spectrometers is steadily growing to match that of the rest of the chemical-ionization world as their use becomes more prevalent. Flexibility in the choice of ion-chemistry has proven benefits by helping to increase selectivity for a number of analytes, providing a variety of reaction products to aid in spectral interpretation, and greatly increasing the versatility of an instrument. However, even with the current palette of ions, most flow-reactor instruments still cannot distinguish between structural isomers such as acetone and propanal or butanone and butanal. Tools capable of making such fine distinctions are therefore being incorporated into newly designed flow-reactor instruments to improve their specificity. Examples can already be found in the literature where gas-chromatography is used for separation prior to CIMS analysis [8] or where a triple–quadrupole mass filter is used for collision-induced dissociation (CID) and fragment ion analysis following chemical-ionization [9]. Other methods of differentiation, such as H/D exchange and analytical ion/molecule reactions with isolated ions, have yet to be applied in air-monitoring flow-reactor instruments.

Much work has been done recently to detect and quantify VOCs emitted by wounded and drying plant material to begin to assess the atmospheric impact of their release on the $HO_x$ budget in the troposphere [8]. Most plants release VOCs following wounding via one or more pathways. The pathway by which wounded plants release C-6 volatiles, such as *cis*-3-hexenal, has been reviewed in-depth by Hatanaka [10]. These compounds are ultimately derived from the enzymatic breakdown of fatty acids following chloroplast disruption. Another family of wound compounds, including carbonyls and HCN, arises from the breakdown of cyanogenic glycosides by enzymes when a cell is ruptured [11]. Both processes are represented in Fig. 1. Studies of such processes provide a convenient testing ground to measure VOCs and HCN with different reagent ions and ion identification techniques in flow-reactor mass spectrometers.

The $OH^-$ anion can be thought of as the negative ion complement to $H_3O^+$. It participates in proton-transfer reactions like $H_3O^+$, but abstracts a proton rather than donating one.

$$H_3O^+ + VOC \rightarrow HVOC^+ + H_2O, \quad PA_{VOC} > PA_{H_2O} \qquad (1)$$

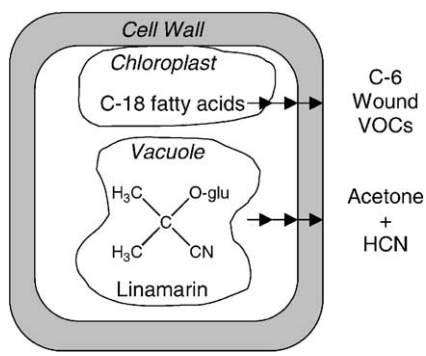


Fig. 1. Wounded or drying plant leaf material can emit numerous VOCs and HCN. C-6 wound VOCs, including hexenals, hexenols, and hexenyl acetates, are produced via several steps following enzymatic breakdown of membrane lipids. HCN and carbonyl compounds are produced as by-products of the two-step decomposition of cyanogenic glycosides following wounding. Linamarin (glu represents glucose), when present in a cyanogenic plant, will give rise to acetone and HCN, while lotaustralin, the ethyl analogue of this compound, will give rise to butanone and HCN.

$$OH^- + VOC \rightarrow (VOC - H)^- + H_2O,$$
$$\Delta H_{acid\,VOC} < \Delta H_{acid\,H_2O} \quad (2)$$

The gas-phase acidity ($\Delta H_{acid}$) of a VOC can be used to determine whether or not it will react with $OH^-$ much as the proton affinity (PA) of a VOC can be used to decide whether it will react with $H_3O^+$. A recent tabulation of proton affinities is given in Hunter and Lias [12], gas-phase acidities in Lide [13], and a short overview of the applicability of such thermochemical data to chemical ionization is given in Bartmess [14]. Like $H_3O^+$, $OH^-$ is simple to generate, reacts at collisional rates with a broad range of organic species, and yields simple ionic products. As with cations, fragment anions generated by CID can often be used to structurally differentiate ions and provide a degree of selectivity in product analysis. A broad overview of tandem mass spectrometry developments and techniques is given in Jennings [15] and is also mentioned in Chapter 3 of Russel [16]. H/D exchange with isolated anions can provide additional structural information about the ions produced. Background on H/D exchange processes and their applicability can be found in Nibbering [17], Hunt and Sethi [18] and, in a more recent application using positive ions, Campbell et al. [19].

In this work, data supporting the use of $OH^-$ anion for negative-ion chemical-ionization of VOCs is reported to expand upon previous studies by Smith and Spanel [6] and Spanel et al. [20]. In addition to reaction rate coefficients, fragment ions resulting from CID of $[M-1]^-$ anions of several VOCs and H/D exchange results for the $[M-1]^-$ anions of the isomeric acetone/propanal and butanone/butanal pairs are also given. These processes were studied as a method of differentiating structural isomers for on-line monitoring. These ion/molecule reaction data are then applied to simultaneous monitoring of acetone, butanone, and HCN released by cyanogenic plants.

## 2. Experimental

All experiments were performed using the tandem FA-SIFT (flowing afterglow-selected ion flow tube) instrument at the University of Colorado at Boulder that has been discussed previously [21]. As pictured in Fig. 2, this instrument consists of an ion source flow-tube, a selection region, a reaction flow-tube, and a detection region. Ions are generated from compounds in the ion source flow-tube through a combination of electron ionization and subsequent ion/molecule reactions. Precursor gases (~0.3 Torr He and trace amounts of other gases) from the ion source are pumped away using a high throughput roots blower

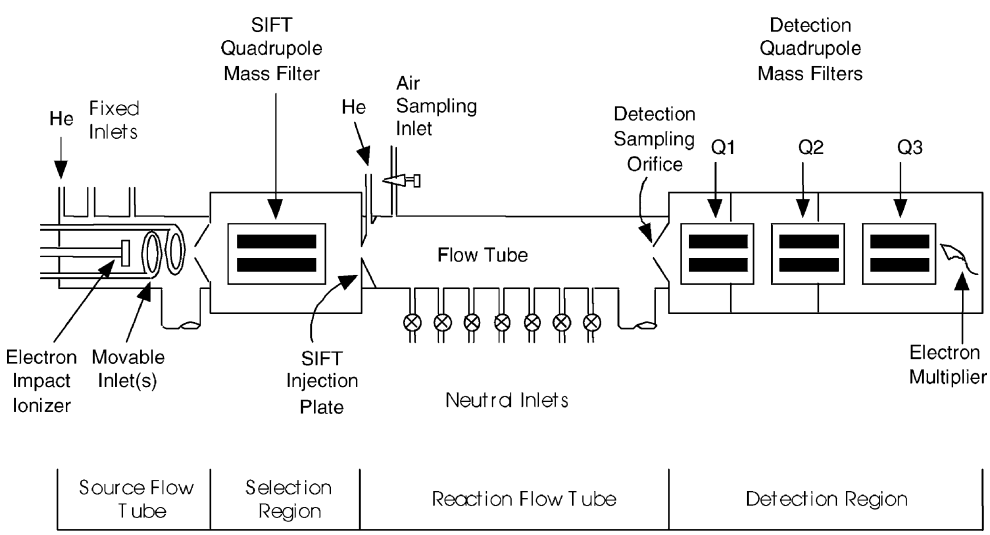


Fig. 2. The tandem flowing-afterglow selected ion flow tube (FA-SIFT) apparatus at the University of Colorado in Boulder.

and mechanical pump and the ions are sampled into the selection region which contains a differentially pumped quadrupole mass filter ($\sim 10^{-4}$ to $10^{-5}$ Torr). Ions of interest are mass selected and then injected into the reaction flow-tube (pressure $\sim$0.5 Torr) with the aid of a venturi inlet. Once in the reaction flow-tube, mass-selected ions can react with pure VOC standards or compounds in sampled air as they flow towards the detection region. Following reaction, gases are pumped away using a second high throughput roots blower and mechanical pump and the final distribution of reagent and product ions is sampled into the differentially pumped detection region ($<10^{-6}$ Torr). Ions are then mass selected using Q3 of a triple–quadrupole mass filter and detected with an electron multiplier.

### 2.1. Generation of $OH^-$, $[M-1]^-$, and $H_3O^+$

To generate $OH^-$ anion, electron ionization of trace amounts of $N_2O$ is used to produce the $O^{\bullet -}$ radical–anion. This anion then abstracts hydrogen from $CH_4$, also added to the ion source, to form the $OH^-$ anion. This anion can be mass selected and injected into the reaction flow-tube or be used to generate other anions of interest while still in the ion source flow-tube.

The $[M-1]^-$ anions of each VOC were generated by adding small flows of the appropriate volatile standard to the ion source downstream of $OH^-$ anion generation. The $OH^-$ anion abstracts a proton from compounds that are more acidic than water to form the $[M-1]^-$ anion with varying yields. These ions can be mass selected and injected into the reaction flow-tube for further study.

The $H_3O^+$ cation was used only for comparison purposes in this study and was generated by electron ionization of trace $H_2O$ added to the ion-source flow-tube.

### 2.2. Collision-induced dissociation by SIFT injection

Multiple collisions with He buffer gas upon injection of $[M-1]^-$ anions into the reaction flow-tube induce CID. This process will be referred to as SIFT–CID hereafter in order to set this process apart from more commonly observed CID experiments performed using triple–quadrupoles, ion-traps, or other devices. The SIFT–CID process has been used and characterized previously in experiments by Kato et al. [22]. The center-of-mass collision energy, and therefore the extent of fragmentation, can be tuned reproducibly during SIFT–CID by changing the SIFT injection voltage. The SIFT injection voltage is defined as the potential difference between the ion-source flow-tube and the SIFT injection-plate. The CID products resulting from this treatment, like other CID experiments, can be very sensitive to the structure of the $[M-1]^-$ anion and can often provide clues to ion identity.

Collision-induced dissociation can also be studied using the triple quadrupole by generating the $[M-1]^-$ anion in the reaction flow-tube, mass selecting the ion with Q1, performing CID in Q2 by addition of a collision gas, and then measuring a mass spectrum using Q3. These experiments were not attempted due to the low $[M-1]^-$ product ion-densities achievable while monitoring trace gases with this instrument. Trace gas monitoring generates product ions in the reaction flow-tube having number densities generally much less than 10% of the reagent ion density for each VOC present. As the maximum $OH^-$ anion signal achievable was 30,000 counts $s^{-1}$, product ion signals rarely exceeded 1000 counts $s^{-1}$. This represents insufficient ion-density to perform a triple–quadrupole CID experiment without significant loss of signal due to ion scattering in the second quadrupole.

Higher $[M-1]^-$ anion number densities can be produced if the instrument is operated as a flowing-afterglow where $OH^-$ anions are generated directly in the reaction flow-tube using electron ionization followed by addition of VOCs or sample air. Although higher $[M-1]^-$ product signals can be obtained for potential triple quadrupole CID studies, this mode of operation also increases background and adds $N_2O$ and $CH_4$ reagents to the reaction region. Normal operation of the instrument using the SIFT quadrupole was preferred and resulted in essentially

zero background at all *m*/*z* of interest with no impurity gases present and provided sufficient sensitivity for our purposes. However, with this mode of operation, SIFT–CID was the only practical method for generating observable fragment ions.

### 2.3. Ion/molecule reaction rate coefficients and reaction products

Ion/molecule reaction rate coefficients and products for reaction between $OH^-$ anion and numerous VOCs were determined. Rate coefficients were measured by adding a constant, calibrated flow of pure reactants through stationary inlets positioned at regular distances along the reaction flow-tube. The slope of a semi-logarithmic plot of reagent anion intensity as a function of reaction distance was used to determine the rate coefficient. A more thorough description of such measurements can be found in Van Doren et al. [23]. Products from reaction of $OH^-$ and each pure standard were determined by recording a mass spectrum over the *m*/*z* range of ∼0–200 while a stable flow of a particular compound was being introduced into the reaction flow-tube. Because of the limited *m*/*z* range recorded, data exists only for those ions up to and including the $[M-1]^-$ anion for most compounds. In most cases, minor amounts of VOC/anion clusters with a *m*/*z* ratio corresponding to $M[M-1]^-$ and $M_2[M-1]^-$ anions were observed and, at least in one case, secondary reaction products were also observed at a mass-to-charge ratio well above that of the $[M-1]^-$ anion. These secondary and association products are not reported here.

### 2.4. H/D exchange

After an $[M-1]^-$ anion has been introduced into the reaction flow-tube it can be allowed to interact with deuterated reagents ($CD_3OD$ in these experiments) added through any of seven inlets along its length. During the course of interaction, H/D exchange between the reagent and the anion will occur with accessible protons and generate a distribution of H/D exchange product ions. This process has been studied in-depth by DePuy et al. [24].

### 2.5. Monitoring of plant VOCs

An inlet far upstream in the reaction region was used to sample air for monitoring plant VOCs. A reaction distance of 93 cm was determined empirically by varying a calibrated flow of isoprene through the sampling inlet while monitoring $OH^-$ anion signal. As the rate coefficient between $OH^-$ and isoprene has previously been measured [25], the reaction distance was used as a variable to fit the known rate coefficient to reagent ion loss and flow rate data. The air-sampling inlet was not heated and consisted of ∼2 cm of 0.63 cm o.d. teflon tubing, a needle valve, a flow meter, and ∼6 cm of 0.63 cm o.d. stainless steel tubing. The Tylan mass flow meter was calibrated with dry room air. No correction for the humidity of the sample air was applied; this correction has been demonstrated elsewhere [26] for mass flow controllers, and would increase measurement accuracy as plant samples generally released high concentrations of water. Periodic measurements of the total flow-tube pressure and temperature near the reaction region were taken to improve concentration estimates where applicable and to demonstrate stability of reaction conditions over the course of an experiment. Sample flow rates were controlled with the needle valve and generally remained at approximately 0.7 STP $cm^3\ s^{-1}$. Once set, the flow rate of air through this inlet varied by less than 2% over a given day. Typical flow-tube pressures ranged from 0.475 to 0.500 Torr. The laboratory temperature near the reaction flow-tube remained at ∼300 K for all experiments.

### 2.6. Plant sample preparation

All plants were grown in the Chemistry Department greenhouses at the University of Colorado in normal potting soil. Plants were periodically fertilized and pesticides were intermittently applied. Several varieties of white clover (*Trifolium repens*) were grown. In addition, cassava (*Manihot esculenta*), eucalyptus (*Eucalyptus polyanthemos*), and cottonwood (*Populus deltoides*) were also grown. Seeds for Dutch white clover were obtained from Arkansas Valley Seed Co. (Lot #021-5413). Other varieties of clover were more

specialized and had been screened or developed previously based on their varying abilities to produce HCN. These varieties and screening studies are mentioned in more detail by Pederson and Brink [27] and Saucy et al. [28]. Seeds for cyanogenic varieties HCNpi and BLHplus as well as acyanogenic BLHminus were generously provided by Gary Pederson of Mississippi State University. Seeds for Aran clover were obtained from the U.S. National Plant Germplasm System, Pullman, WA. Seeds for Ladino clover were obtained from Germinal Holdings Ltd., Banbridge, N. Ireland.

Plant samples were prepared by cutting approximately 3–5 g of fresh plant material, including leaves and stems, from trays in the greenhouse. Plants were sampled at various seasons of the year but were generally cut in the morning without regard to prior fertilization, watering, or application of pesticides. Plant clippings were weighed and then wounded by freezing in liquid nitrogen. This treatment has been shown to provide homogeneous wounding by rupturing cell walls through the freezing and expansion of water inside each plant cell. Upon thawing, any VOCs stored in the plant cells are liberated, as are VOCs immediately generated by the action of wounding if enzymatic production has not been disrupted by the liquid nitrogen treatment. Polyethylene bags of ~1 L volume and 0.6 mm thickness were used as sampling chambers where frozen, wounded plant material could thaw. Sample bags were filled with room air using a hand-pump prior to thawing and were generally prepared about an hour before sampling. Larger plant samples in a glass flask were used when generating $[M-1]^-$ anions directly in the ion-source flow-tube for subsequent H/D exchange analysis. Empty sample bags and flasks were tested to account for any background arising from the polyethylene and glass surfaces or the room air used.

### 2.7. Compound sources and purities

The following is a list of compounds, vendors, and the quoted purity for all volatile standards tested. Compounds were used without further purification. Acetone, Fisher, 99.60%; propanal, Lancaster, 97%; butanal, Lancaster, 99%; butanone, Fisher, 99.70%; isoprene, Aldrich, 99%; 2-methyl-3-buten-2-ol, Aldrich, 98%; 3-methyl-2-butene-1-ol, Aldrich, 99%; (*Z*)-3-hexenyl acetate, Bedoukian, not listed; (*E*)-2-hexenyl acetate, Aldrich, 98%; (*Z*)-3-hexen-1-ol, Aldrich, 98%; (*E*)-2-hexen-1-ol, Aldrich, 96%; (*E*)-3-hexen-1-ol, Lancaster, 97%; *n*-hexanal, Aldrich, 98%; (*Z*)-3-hexenal, Bedoukian, 50% in triacetin; (*E*)-2-hexenal, Aldrich, 98%; hexyl acetate, Aldrich, 99%; hexyl alcohol, Aldrich, 98%; $CD_3OD$, Cambridge Isotope Laboratories, 99.8%.

## 3. Results and discussion

### 3.1. Ion/molecule reaction studies

The ion-chemistry presented here provides useful information for quantifying and identifying many biogenic wound VOCs and for distinguishing some of their structural isomers. A few of the compounds tested are not wound compounds specifically but are included to add to the ion-chemistry database for future reference.

#### 3.1.1. Rate coefficients

A summary of measured reaction rate coefficients, rate coefficients calculated using the parameterized trajectory collision theory of Su and Chesnavich [29], and rate coefficients found in Ikezoe et al. [30] for the reaction between $OH^-$ and each VOC is given in Table 1. For comparison, complementary data for $H_3O^+$ are given in Table 2. Original citations for literature values are: HCN (with $H_3O^+$ [31], with $OH^-$ [32]), acetone (with both $H_3O^+$ and $OH^-$ [33]), isoprene (with $OH^-$ [25]), hexenals (with both $H_3O^+$ and $OH^-$ [20]), and hexyl alcohol (with $H_3O^+$ [34]). Dipole moments and polarizabilities used in calculating rate coefficients are listed in Table 3. Where dipole moments were unavailable in Lide [35], they were estimated based on homologous series of compounds with known values. Where polarizabilities were unavailable, they were estimated based on the methods of Miller and Savchik [36].

Table 1
Reaction rate coefficients for $OH^-$ reacting with VOCs and HCN

| Compound | $OH^-$ [a] ($\times 10^{-9}$ cm$^3$ molecule$^{-1}$ s$^{-1}$) | Collision rate[b] ($\times 10^{-9}$ cm$^3$ molecule$^{-1}$ s$^{-1}$) | Lit.[a,c] ($\times 10^{-9}$ cm$^3$ molecule$^{-1}$ s$^{-1}$) |
|---|---|---|---|
| Hydrogen cyanide | N | 4.3 | 3.5 ± 0.7 |
| Propanal | 3.2 ± 0.5 | 3.9 | N |
| Acetone | 3.5 ± 0.8 | 4.1 | 3.7 ± 0.9 |
| Butanal | 3.2 ± 0.7 | 4.0 | N |
| 2-Butanone | 3.5 ± 0.5 | 4.0 | N |
| Isoprene | 1.8 ± 0.4 | 2.1 | 1.3 |
| 2-Methyl-3-buten-2-ol | 2.5 ± 0.4 | 3.2 | N |
| 3-Methyl-2-buten-1-ol | 2.8 ± 0.5 | 3.2 | N |
| *trans*-2-Hexenal | ∼3[d] | 4.1 | ∼4 |
| *cis*-3-Hexenal | ∼5[d] | 4.1 | ∼4 |
| *cis*-3-Hexen-1-ol | ∼2[d] | 3.1 | N |
| *trans*-2-Hexen-1-ol | ∼3[d] | 3.1 | N |
| *trans*-3-Hexen-1-ol | 2.4 ± 0.3 | 3.1 | N |
| *n*-Hexanal | 3.3 ± 0.6 | 4.1 | N |
| Hexyl alcohol | 2.8 ± 0.5 | 3.0 | N |
| Hexyl acetate | 2.9 ± 0.4 | 3.4 | N |
| *trans*-2-Hexenyl acetate | 2.8 ± 0.4 | 3.4 | N |
| *cis*-3-Hexenyl acetate | 3.0 ± 0.4 | 3.4 | N |

[a] "N" indicates that the VOC was not studied or that no literature value could be found.
[b] Rate coefficients were calculated by the parameterized trajectory collision theory of Su and Chesnavich [29], using polarizability and dipole-moment values from Table 3.
[c] Literature values were mainly taken from Ikezoe et al. [30]. Original citations are also given in the main text (Section 3.1.1).
[d] Where uncertainties are omitted, changes in compound flow rates caused a systematic variation in the rate coefficient measurement.

All measured rate coefficients are averages of at least three independent rate determinations. The lack of reported uncertainties for the *cis*-3- and *trans*-2-hexenal, as well as *trans*-2-hexen-1-ol and *cis*-3-hexen-1-ol rate coefficients, reflects systematic instabilities in neutral flow rates encountered during measurement. These instabilities were also reported by Spanel et al. [20] following attempts to measure reaction rate coefficients with *cis*-3- and *trans*-2-hexenal. All measured rates are close to the calculated, collisional values, demonstrating that the negative CI reactions are as efficient as proton-transfer reactions using $H_3O^+$. Due to the uniform efficiency of these reactions, either measured or calculated values may be used for quantification of VOCs.

### 3.1.2. Reaction products

Reaction products for the reaction of each compound with $OH^-$ are listed in Table 4 based on their relative peak heights taken from a mass spectrum. Complementary data for reaction with $H_3O^+$ are given in Table 5 for comparison. Minor products have peak intensities less than half those of major peaks. The numbers in these tables should be used as a general guideline for ion masses that are produced by reaction between $OH^-$ and a given VOC rather than as a definitive list of peak-heights and ion *m*/*z* ratios which will appear during trace gas monitoring. Under the experimental conditions, association reactions generated ions with *m*/*z* up to $M_2[M-1]^-$ for some compounds. Secondary reactions between product anions and excess neutral carbonyl compounds, identical to those reported by Sheldon et al. [37], were observed in a test of benzaldehyde although the results are not reported here. It also seems reasonable that gas-phase base-catalyzed Claisen–Schmidt reactions might occur as reported by Haas and Gross [38] although these products were not studied specifically and should be indistinguishable from the association product. Association and secondary processes should

Table 2
Reaction rate coefficients for $H_3O^+$ reacting with VOCs and HCN

| Compound | $H_3O^+$ [a] ($\times 10^{-9}$ cm$^3$ molecule$^{-1}$ s$^{-1}$) | Collision rate[b] ($\times 10^{-9}$ cm$^3$ molecule$^{-1}$ s$^{-1}$) | Lit.[a,c] ($\times 10^{-9}$ cm$^3$ molecule$^{-1}$ s$^{-1}$) |
|---|---|---|---|
| Hydrogen cyanide | N | 4.2 | 3.5 ± 0.7 |
| Propanal | N | 3.8 | N |
| Acetone | N | 3.9 | 3.9 ± 0.9 |
| Butanal | 3.6 ± 0.6 | 3.8 | N |
| 2-Butanone | 3.3 ± 0.6 | 3.9 | N |
| Isoprene | N | 2.0 | N |
| 2-Methyl-3-buten-2-ol | 2.2 ± 0.4 | 3.1 | N |
| 3-Methyl-2-buten-1-ol | 2.7 ± 0.5 | 3.1 | N |
| *trans*-2-Hexenal | ∼4[d] | 3.9 | ∼4 |
| *cis*-3-Hexenal | ∼3[d] | 3.9 | ∼4 |
| *cis*-3-Hexen-1-ol | 2.8 ± 0.5 | 2.9 | N |
| *trans*-2-Hexen-1-ol | ∼3[d] | 2.9 | N |
| *trans*-3-Hexen-1-ol | 2.5 ± 0.4 | 2.9 | N |
| *n*-Hexanal | 3.4 ± 0.7 | 3.9 | N |
| Hexyl alcohol | 2.6 ± 0.5 | 2.9 | 2.9 |
| Hexyl acetate | 3.2 ± 0.6 | 3.3 | N |
| *trans*-2-Hexenyl acetate | 3.1 ± 0.5 | 3.2 | N |
| *cis*-3-Hexenyl acetate | 3.2 ± 0.5 | 3.2 | N |

[a] "N" indicates that the VOC was not studied or that no literature value could be found.
[b] Rate coefficients were calculated by the parameterized trajectory collision theory of Su and Chesnavich [29], using polarizability and dipole-moment values from Table 3.
[c] Literature values were mainly taken from Ikezoe et al. [30]. Original citations from this work are given in the main text (Section 3.1.1).
[d] Where uncertainties are omitted, changes in VOC flow rates caused a systematic variation in the rate coefficient measurement.

not be observable under rigorous trace-gas monitoring conditions in which the neutral concentrations are substantially lower. High water concentrations encountered during most air-monitoring experiments will also change relative peak heights from those reported in the table. Mass discrimination effects are constant for all reaction product measurements and should not affect the gross features of these results.

Proton abstraction reactions involving $OH^-$ produce a range and diversity of ions similar to that produced by proton transfer reactions involving $H_3O^+$. An in-depth analysis of ionic products resulting from each reaction is beyond the scope of this work. The interested reader is referred to the first chapter of Russel [16] and references therein for discussion of decomposition of $[M-1]^-$ anions as many of the minor peaks can be attributed to the breakdown of these anions. This includes examples showing losses of $H_2$ to form $[M-3]^-$ anions, $CH_4$ to form $[M-17]^-$ anions, $H_2O$ to form $[M-19]^-$ anions, $C_2H_4$ (or CO) to form $[M-29]^-$ anions, and $C_2H_6$ (or $H_2CO$) to form $[M-31]^-$ anions which are all observed in Table 4. Characteristic product ions such as *m*/*z* 59, presumably the anion of acetic acid, are observed when testing compounds containing an acetate group. Characteristic fragment ions such as *m*/*z* 41, an anion produced by many different compounds and often corresponding to the $HC_2O^-$ anion, are also observed.

Even in this relatively small subset of biogenic VOCs, there are numerous compounds producing major ions whose *m*/*z* ratios overlap following reaction with $OH^-$. For example, acetone and propanal, butanone and butanal, *trans*-2- and *cis*-3-hexenal, and *trans*-2- and *cis*-3-hexenyl acetate fall into this category. Although minor ions may provide a method of positive identification, for example *trans*-2-hexenal and *cis*-3-hexenal might be distinguished by the appearance of an ion at *m*/*z* 69, minor ions may not be observable or may overlap with other ions in the presence of complex mixture of VOCs. If a minor ion is

Table 3
Polarizability and dipole moment values for VOCs and HCN

| Compound | Polarizability[a,b] ($\times 10^{-24}$ cm$^3$) | Dipole moment[a,c] (D) |
|---|---|---|
| Hydrogen cyanide | 2.53 | 2.99 |
| Propanal | 6.5 | 2.72 |
| Acetone | 6.37 | 2.88 |
| Butanal | 8.2 | 2.72 |
| 2-Butanone | 8.13 | 2.78 |
| Isoprene | 9.99 | 0.25 |
| 2-Methyl-3-buten-2-ol | 10.4 | 1.9 |
| 3-Methyl-2-buten-1-ol | 10.4 | 1.9 |
| *trans*-2-Hexenal | 11.6 | 2.7 |
| *cis*-3-Hexenal | 11.6 | 2.7 |
| *cis*-3-Hexen-1-ol | 12.2 | 1.7 |
| *trans*-2-Hexen-1-ol | 12.2 | 1.7 |
| *trans*-3-Hexen-1-ol | 12.2 | 1.7 |
| *n*-Hexanal | 11.9 | 2.7 |
| Hexyl alcohol | 12.5 | 1.6 |
| Hexyl acetate | 16.2 | 1.9 |
| *trans*-2-Hexenyl acetate | 16 | 1.9 |
| *cis*-3-Hexenyl acetate | 16 | 1.9 |

[a] Where multiple values were found in Lide [35], the average value was taken.
[b] Where no polarizability values were available, they were estimated using the method of Miller and Savchik [36].
[c] Where no dipole-moment values were available, they were estimated based on homologous series of compounds.

used to quantify a VOC, the overall sensitivity of the technique is limited by its measurement since it must either be used directly for quantification or for determining the fraction of a more abundant ion due to an individual compound. Other methods are needed to provide structural information when minor peaks are not available or otherwise suspect for identification purposes.

### 3.1.3. CID products

Fragmentation products of $[M-1]^-$ anions are listed in Table 6 based on their relative peak heights in a mass spectrum. Minor products have peak heights less than half that of major peaks. Often, only a low density of $[M-1]^-$ ions could be introduced into the reaction flow-tube following ion-generation and mass selection. When the parent $[M-1]^-$ ion was not abundant, fragment ions were often only slightly above the background of around 0–4 counts s$^{-1}$. Only those peaks are reported which had a peak height at

Table 4
Products of the reaction between $OH^-$ anion and volatile standards and HCN

| Compound | Major products (*m*/*z*) | Minor products[a,b] (*m*/*z*) |
|---|---|---|
| Hydrogen cyanide | 26 | N |
| Propanal | 57 | N |
| Acetone | 57 | N |
| Butanal | 71 | N |
| 2-Butanone | 71 | N |
| Isoprene | 67 | 41, 39 |
| 2-Methyl-3-buten-2-ol | 85 | 69, 57 |
| 3-Methyl-2-buten-1-ol | 85, 67 | 83, 45, 35 |
| *trans*-2-Hexenal | 97 | 45 |
| *cis*-3-Hexenal | 97 | 69, 45 |
| *cis*-3-Hexen-1-ol | 99 | 81, 69, 35 |
| *trans*-2-Hexen-1-ol | 99 | 97, 81, 35 |
| *trans*-3-Hexen-1-ol | 99, 35 | 97, 81, 71, 69, 57, 45 |
| *n*-Hexanal | 99 | N |
| Hexyl alcohol | 101 | N |
| Hexyl acetate | 143, 59 | N |
| *trans*-2-Hexenyl acetate | 59 | 141, 41 |
| *cis*-3-Hexenyl acetate | 59 | 141, 77, 41 |

[a] Minor products are less than half the intensity of major products.
[b] "N" indicates that no minor products were observed.

Table 5
Products from the reaction between $H_3O^+$ cation and volatile standards and HCN

| Compound | Major products (*m*/*z*) | Minor products[a,b] (*m*/*z*) |
|---|---|---|
| Hydrogen cyanide | N | N |
| Propanal | N | N |
| Acetone | N | N |
| Butanal | 73 | 55, 43 |
| 2-Butanone | 73 | 43 |
| Isoprene | N | N |
| 2-Methyl-3-buten-2-ol | 81, 69 | 87 |
| 3-Methyl-2-buten-1-ol | 81, 69 | 85 |
| *trans*-2-Hexenal | 99 | 81, 57, 47 |
| *cis*-3-Hexenal | 99, 81 | 71, 69, 47, 43 |
| *cis*-3-Hexen-1-ol | 83 | 101, 99, 67 |
| *trans*-2-Hexen-1-ol | 83, 81 | 101, 99, 95 |
| *trans*-3-Hexen-1-ol | 83 | 101, 99, 69 |
| *n*-Hexanal | 101, 83 | 33 |
| Hexyl alcohol | 85 | 87, 86 |
| Hexyl acetate | 61 | 145, 85 |
| *trans*-2-Hexenyl acetate | 83 | 143, 61, 33 |
| *cis*-3-Hexenyl acetate | 143, 83 | 61 |

[a] Minor products are less than half the intensity of major products.
[b] "N" indicates that the compound was not tested or that no minor products were observed.

Table 6
Fragment ions observed following SIFT–CID of the $[M-1]^-$ ion of each VOC

| Compound | $[M-1]^-$ injected (*m*/*z*) | $V_{inj}$[a] (V) | Major fragment (*m*/*z*) | Minor fragment[b] (*m*/*z*) |
|---|---|---|---|---|
| Hydrogen cyanide | N | N | N | N[c] |
| Propanal | 57 | 40 | 57 | 55, 41, 27, 17 |
| Acetone | 57 | 40 | 57, 41 | 39, 17 |
| Butanal | 71 | 40 | 71 | 69, 55, 43, 41, 27, 25, 17 |
| 2-Butanone | 71 | 40 | 71 | 69, 55, 43, 41, 27, 17 |
| Isoprene | 67 | 30 | 67 | N |
| 2-Methyl-3-buten-2-ol | 85 | 30 | 57 | 85, 69, 41, 27, 17 |
| 3-Methyl-2-buten-1-ol | 85 | 30 | 67 | 85, 57, 55, 27, 17 |
| *trans*-2-Hexenal | 97 | 40 | 97 | 95, 82, 69, 67, 55, 53, 43, 41 |
| *cis*-3-Hexenal | 97 | 40 | 97 | 95, 82, 69, 67, 55, 43, 41, 27, 17 |
| *cis*-3-Hexen-1-ol | 99 | 40 | 69 | 99, 97, 17 |
| *trans*-2-Hexen-1-ol | 99 | 40 | 97 | 99, 71, 69, 17 |
| *trans*-3-Hexen-1-ol | 99 | 40 | 69 | 99, 97, 43, 17 |
| *n*-Hexanal | 99 | 40 | 99 | 97, 71, 57, 55, 43, 41, 27, 17 |
| Hexyl alcohol | 101 | 40 | 99 | 101 |
| Hexyl acetate | 143 | 40 | 41 | 143 |
| *trans*-2-Hexenyl acetate | 141 | 40 | 41 | 141, 72, 69 |
| *cis*-3-Hexenyl acetate | 141 | 40 | 41 | 141, 111, 59 |

[a] The injection voltage is defined as the potential difference between the source flow-tube and the SIFT injection plate. The injection voltage correlates with the center-of-mass collision energy as observed during previous studies [22].
[b] Minor products are less than half the intensity of major products.
[c] Although HCN was not studied, the $CN^-$ anion is very stable and will not dissociate under our SIFT-injection conditions.

least double that of the background noise (S/N of 2:1). Under more favorable fragmentation conditions, additional fragment ions might be observed. Unlike measurement of reaction products, no excess neutral carbonyl was available in the reaction flow-tube to undergo clustering or secondary reactions with the $[M-1]^-$ anion being tested. The only other interferences arise from insufficient mass selection for larger anions with the SIFT quadrupole or persistent contamination of the ion source inlets with isomeric compounds during a previous experiment. For the majority of the $[M-1]^-$ anions tested, clean mass selection was easily achievable as the ion of interest was separated from all other ions by at least 2 mass units and the selection region quadrupole was operated with a resolution of at least 1 mass unit. During these experiments, care was taken to avoid using compounds that would produce $[M-1]^-$ anions with identical *m*/*z* during back-to-back experiments, through the same inlet, or even on the same day to minimize interference by structural isomers.

Fragment ion products show some similarities to the simple $OH^-$ reaction products, although the two are rarely identical. For a more in-depth discussion of mechanisms of CID, the reader is again referred to the first chapter of Russel [16] and the references therein. Variable amounts of the $[M-1]^-$ anion remain intact following SIFT–CID for most compounds. A large increase in the occurrence of the $[M-3]^-$ (loss of $H_2$) ion is also observed compared to simple $OH^-$ reaction products. Characteristic ion pairs separated by *m*/*z* of 2 (for example, *m*/*z* 69 and 67, or *m*/*z* 55 and 53, or *m*/*z* 43 and 41) are also frequently observed. The hydroxide anion, *m*/*z* 17 ($OH^-$), is also often generated in small amounts. This anion possibly arises from the carbonyl oxygen as no residual $OH^-$ from the ion source reaches the main reaction flow-tube following mass selection of an $[M-1]^-$ anion. However, no systematic testing of oxygenated versus non-oxygenated compounds was performed to explore this issue.

Compounds such as acetone and propanal, whose simple reaction products are almost identical, can be

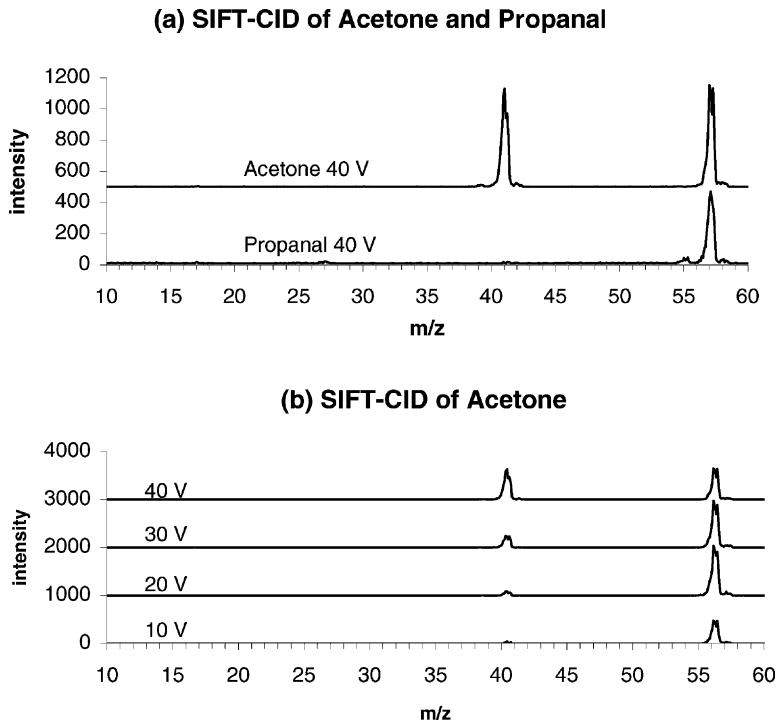


Fig. 3. (a) Fragment ions following SIFT–CID of *m*/*z* 57 generated using acetone and propanal. Anions derived from these compounds can be distinguished based on the peak height of *m*/*z* 41. (b) SIFT–CID of *m*/*z* 57 generated using an acetone standard. Variation of the SIFT injection voltage, defined as the potential difference between the ion-source flow tube and the SIFT injection plate, can be used to systematically change the relative peak height of the fragment at *m*/*z* 41.

distinguished based on their characteristic fragment ions (Fig. 3a). Even compounds that generate identical fragment ions, such as *m*/*z* 69 which arises from *cis*-3- and *trans*-2-hexenal, can be distinguished based on peak heights under reproducible SIFT–CID conditions as was shown in previous work [39]. Relative peak heights can be controlled reproducibly by variation of the injection voltage, which correlates with the center-of-mass collision energy (Fig. 3b). In the case of acetone and propanal, the anion at *m*/*z* 41 arises through the loss of methane via the methyl radical which is facile for the enolate anion of acetone but not so for that of propanal (Fig. 4a). In the case of *trans*-2- and *cis*-3-hexenal, the minor peak at *m*/*z* 69 is more abundant for *trans*-2-hexenal and allows these compounds to be distinguished. The greater abundance of *m*/*z* 69 in *trans*-2-hexenal arises from loss of CO, presumably following deprotonation of some percentage of these molecules at the acyl hydrogen followed by rearrangement to a more stable anion (Fig. 4b). This hydrogen is generally not accessible to abstraction using $OH^-$ anion as can be seen in acetaldehyde which has a gas-phase acidity of ∼390 kcal/mol [40] (Fig. 4b), identical to that of water. The gas-phase acidity of this site on *trans*-2-hexenal is made accessible to proton abstraction by $OH^-$ through the proximity of the C–C double bond α to the carbonyl carbon. In *cis*-3-hexenal, the double bond is further away and does not favorably affect the gas-phase acidity of its acyl hydrogen. The gas-phase acidity of the analogous hydrogen in acrolein has not been measured to show the effect of a double bond on the gas-phase acidity of the acyl hydrogen. The gas-phase acidity of the hydrogen on the carbon atom α to the carbonyl carbon (Fig. 4b), however, has been measured as 375 kcal/mol [41] and has been shown to be

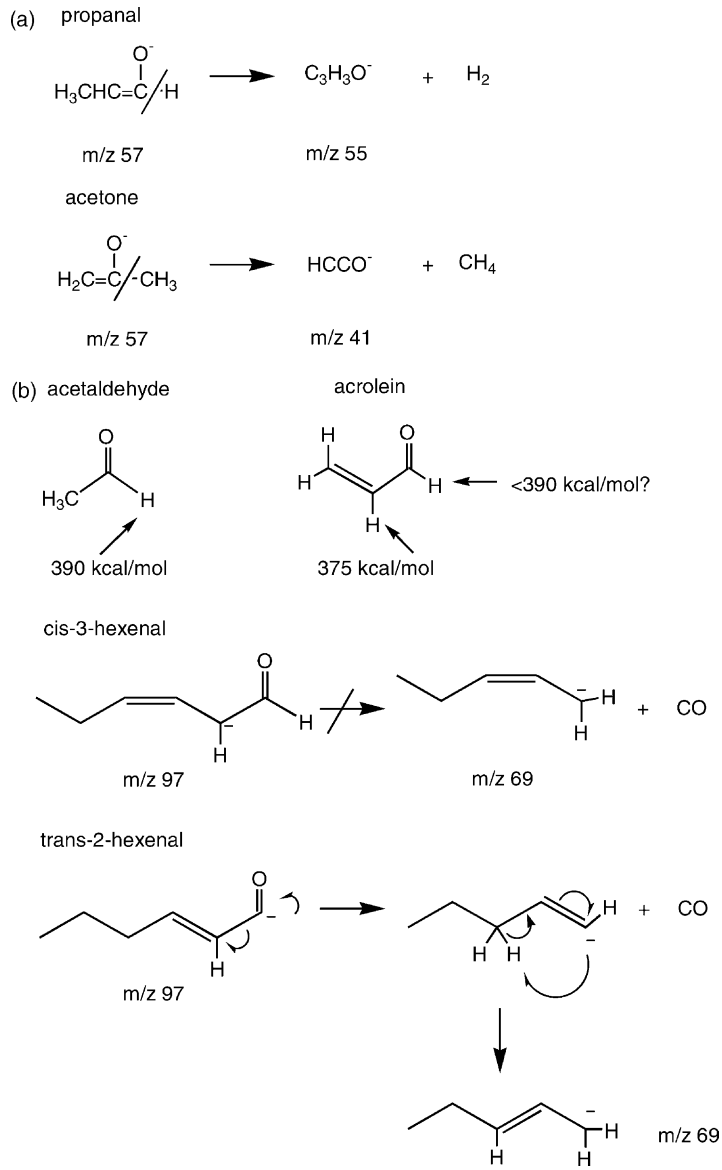


Fig. 4. (a) Acetone and propanal enolate ions lose methane and hydrogen, respectively. This loss accounts for the greater abundance of the *m*/*z* 41 fragment ion of the $[M-1]^-$ anion of acetone. (b) The hydrogen atom α to the carbonyl carbon is abstracted from *cis*-3- and *trans*-2-hexenal following reaction with $OH^-$. However, the *trans*-2-hexenal $[M-1]^-$ acyl anion also forms and may undergo loss of CO.

the main site of deprotonation [42]. It is likely that deprotonation of *trans*-2-hexenal is also favored at this site or sites α to the double bond on the opposite side from the carbonyl carbon. However, the acidity of the acyl hydrogen will be decreased sufficiently below 390 kcal/mol that some percentage will be abstracted by $OH^-$. Increased abundance of this specific ion will give rise to CID resulting in loss of CO and a higher fragment peak at *m*/*z* 69. Additional support for this mechanism is that loss of CO has been observed from a dimer of the acrolein $[M-1]^-$ anion [42].

SIFT–CID fragment ions are indispensable for distinguishing many of the isomeric compounds listed here. This analysis is somewhat simpler than relying on observation of minor reaction products since the parent $[M-1]^-$ anion is isolated from the complex sample matrix prior to SIFT–CID. The resulting fragment ions cannot be confused with other, simultaneous ion/molecule reaction products. Isolation of a single ion does not provide for the fact that different neutral precursors might generate identical anions, for example 2-methyl-3-butene-2-ol and acetone have different molecular weights but both produce an ion at *m*/*z* 57. However, isolation of an anion does open the door to other methods of distinguishing isomeric ions such as the use of ion/molecule reactions capable of probing ion structure.

#### 3.1.4. H/D exchange

The isomeric $[M-1]^-$ ions generated using pure acetone and propanal as well as butanone and butanal standards were reacted with $CD_3OD$ to probe the number of hydrogen atoms that would be exchanged with deuterium. As expected, based on proximity to the carbonyl carbon and acidities of hydrogen atoms, propanal and butanal exchanged a single proton and only in small yield. The ketone anions exchanged up to the total number of hydrogen atoms as observed previously by DePuy et al. [24].

In order to observe full exchange, excess $CD_3OD$ must be added to the reaction region. Due to high concentrations of these species in the reaction region, both deuterium exchange reactions with the deuterated reagents (3) and association reactions (4) are observed simultaneously.

$$CH_3C(O)CH_2^- + CD_3OD \rightarrow CH_3C(O)CHD^- + CD_3OH \quad (3)$$

$$CH_3C(O)CHD^- + CD_3OD \xrightarrow{He} CH_3C(O)CHD^-(CD_3OD) \quad (4)$$

Mass spectra for $[M-1]^-$ anions of acetone and propanal following H/D exchange and association reactions with $CD_3OD$ appear in Fig. 5a and b. Ionic H/D exchange products are observed at the *m*/*z* of the $[M-1]^-$ anion as well as the *m*/*z* of the $[M-1]^-$ anion plus that of $CD_3OD$. Ratios of peak heights for clustered ions such as 94/93 (for the acetone/propanal pair) and 108/107 (for the butanone/butanal pair) can be used as sensitive indicators of whether an aldehyde, a ketone, or a mixture of the two is present while generating an $[M-1]^-$ anion during air monitoring. This ratio is given for pure acetone, propanal, butanone, and butanal in Fig. 6 using a single flow rate of $CD_3OD$.

### 3.2. Application to cyanogenic plants

As mentioned in Section 1, a variety of green plants produce cyanogenic glycosides that give rise to volatile carbonyls and HCN upon leaf wounding. In this work we extend earlier studies applying negative ion CIMS using $OH^-$ to the analysis of headspace gases from wounded cyanogenic and acyanogenic plants [39] to the simultaneous detection of HCN, acetone, and butanone. These compounds should be released following breakdown of linamarin (acetone and HCN) and lotaustralin (butanone and HCN), respectively (Fig. 1), and are seldom measured simultaneously or with a single instrument. Plant headspace measurements were alternated with measurements of room-air bubbled through water in order to match humidity conditions and test the lab air for background impurities. These alternating samples, measured during a single experiment, are shown in Fig. 7. During a typical experiment, the $OH^-$ reagent ion generally decreased over time as the ion-source drifted, but never decreased by more than 6% due to reaction with VOCs. Large variations in water concentration occurred following sampling of cassava and cottonwood due to limitations in the sample size. Aside from these plants, water concentrations remained approximately constant throughout a given experiment, even between plant samples and blank, humidified air samples. Results were highly reproducible and did not seem to be affected by watering, fertilizing, or application of pesticides to the plants, although this was not investigated systematically. The thawing time and the time between cutting and freezing of plant

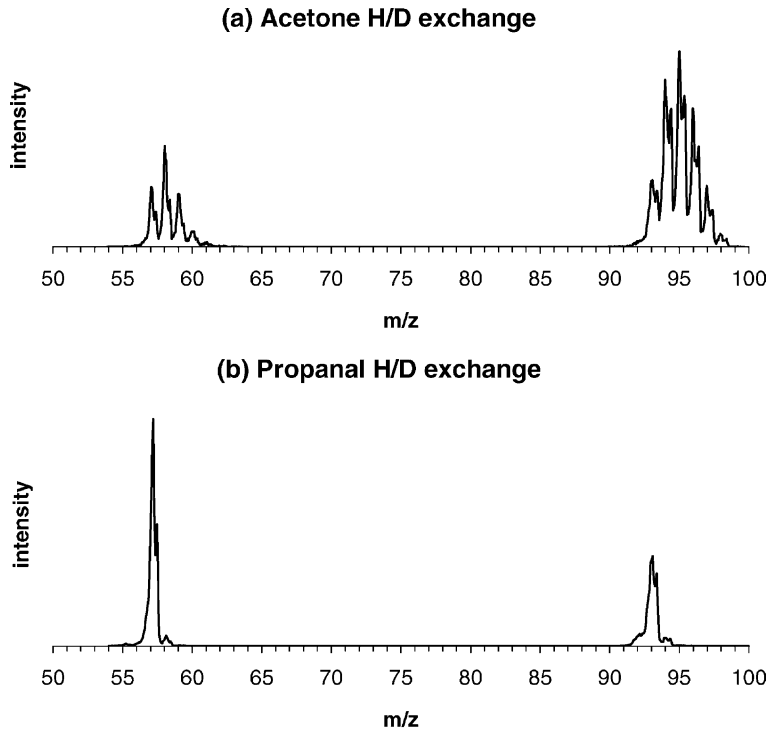


Fig. 5. (a) Acetone $[M-1]^-$ anion participates in H/D exchange and association with $CD_3OD$. Up to five exchanges are observed. (b) Propanal $[M-1]^-$ anion participates in H/D exchange and association reactions with $CD_3OD$. Only a single exchange is observed.

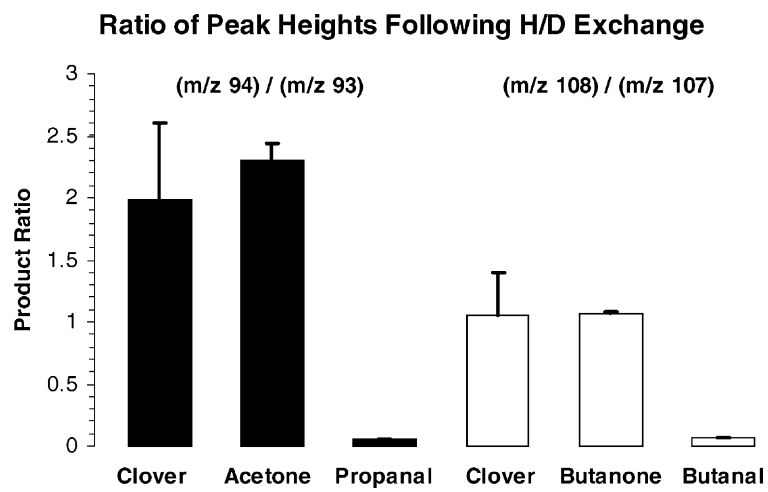


Fig. 6. Ratios of $CH_3C(O)CHD^-(CD_3OD)$ to $CH_3C(O)CH_2^-(CD_3OD)$ peak heights and $CH_3CH_2C(O)CH_2^-(CD_3OD)$ to $CH_3CH_2C(O)CD^-(CD_3OD)$ peak heights observed using acetone, propanal, butanone, and butanal standards to generate the initial $[M-1]^-$ anion (*m*/*z* 57 for acetone and *m*/*z* 71 for butanone). These ratios are also given using an HCNpi clover sample to generate the initial $[M-1]^-$ anion. These results, including estimated uncertainties, suggest that acetone and butanone are the main species emitted.

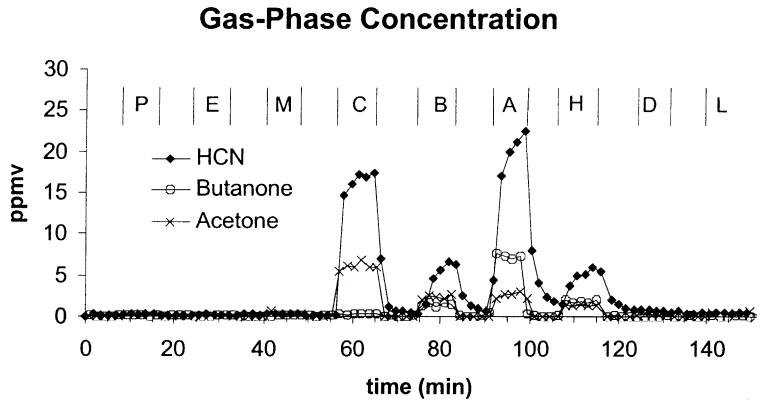


Fig. 7. Mixing ratios of acetone, butanone, and HCN observed in sample headspace for nine different plants. Acyanogenic species included: P, cottonwood (*Populus deltoides*), 2.17 g; E, eucalyptus (*Eucalyptus polyanthemos*), 0.57 g; M, BLHminus clover, 0.19 g; D, Dutch white clover, 0.15 g; L, Ladino clover, 0.17 g. Cyanogenic species included: C, cassava (*Manihot esculenta*), 0.01 g; B, BLHplus clover, 0.20 g; A, Aran clover, 0.19 g; H, HCNpi clover, 0.25 g. A blank of humidified room air is sampled between plant experiments.

material also did not seem to affect the magnitude or character of the plant emissions. No emissions from empty polyethylene bags or the glass sampling chamber were detected in separate experiments, although room air often contained a small amount of water and sometimes generated trace amounts of $O_2^-$ at *m*/*z* 32.

Ion signals can be converted to mixing ratios in the sample bag using the simple model given by the expression:

$$[\mathrm{VOC}] = -\left(\frac{1}{kt}\right)\ln\left(\frac{[\mathrm{OH}^-]_t}{[\mathrm{OH}^-]_0}\right) \quad (5)$$

The variable [VOC] is the concentration of neutral VOC molecules in the reaction region (molecule $cm^{-3}$), $k$ the reaction rate coefficient ($cm^3$ molecule$^{-1}$ $s^{-1}$), $t$ the reaction time (s), $[OH^-]_t$ the reagent ion concentration following reaction with the VOC in question (molecule $cm^{-3}$), and $[OH^-]_0$ is the reagent ion concentration before reaction. Reaction time can be calculated based on flow, pressure, temperature, and reaction distance measurements and these same measured variables can be used to calculate the mixing ratio of the VOC in the sampled air.

The total reagent ion signal was assumed to consist of the sum of the $OH^-(H_2O)_{0,1,2}$ cluster ions at *m*/*z* 17, 35, and 53 due to the humidity of the sampled air. A small amount of *m*/*z* 71 ($OH^-(H_2O)_3$) could also be observed but was negligible in comparison to the other adduct ions. The ratio of cluster ions $OH^-(H_2O)_n$ for $n = 0, 1, 2, 3$ with respect to their sum was generally near $98.5{:}1.4{:}0.1{:}0.0_1$. Additionally, each of the cluster ions, $n > 0$, is assumed to react with a particular VOC at the same rate as the bare $OH^-$ anion so that only one reaction rate coefficient needs to be used for quantification of a given VOC. Rate coefficients for the reaction between $OH^-(H_2O)_n$ anions and several species have been measured experimentally [43]. These studies show a decrease in the reaction rate coefficient with increasing n that depends on the nature of the reacting species. Rate coefficients begin to drop rapidly for reaction between $OH^-(H_2O)_n$ and $CO_2$ [44] and HBr [45] beginning at $n = 4$ and 8, respectively. The reaction rate with acetone [46] decreases rapidly at $n = 2$. Since the most abundant reactant ions in our system are $n = 0$ and 1, only a small error is expected from using the rate constant for $n = 0$ and applying this to all species. Further, it is unlikely that reaction products different from those observed when exclusively $n = 0$ is present will be produced under these conditions. The varying amounts of water released by each plant sample should not drastically affect quantification results for our purposes here, although it may be a significant effect if high accuracy is desired. Mass discrimination and

differential diffusion were also not taken into account for these measurements. Corrections for humidity, mass discrimination, and differential diffusion have been discussed by Spanel and Smith [47]. In our study, however, most ions are relatively small ($m/z < 100$) so that corrections would not be large.

Total product ion signal generally consists of the sum of the base $[M-1]^-$ ion and the first water cluster. The natural isotopic abundance of each ion or any possible minor fragments were not included although they are needed for more exact quantification in the absence of empirical calibration. The sum of the total parent ion signal and the total product ion signal for a given compound was used as the total parent signal prior to reaction, given as $[OH^-]_0$ in Eq. (5).

Fig. 7 is a plot of acetone, butanone, and HCN released by nine different plants. All plants were tested during a single experimental effort in order to maintain consistent reaction conditions and to simplify intercomparison of results. Variation in sample sizes is largely due to difficulties in weighing exact masses into sample bags before leaf material began to thaw and adhere to surfaces, although sample weights for cottonwood, eucalyptus, and cassava were chosen for the convenient headspace concentration of VOCs produced. Different letters in Fig. 7 identify the plant being studied and show the general time during which each sample was present on the sampling inlet.

Only known cyanogenic plants, including cassava, BLHplus, Aran and HCNpi clover, produced simultaneous signals for HCN, acetone, and butanone. Acyanogenic plants showed only background signals for these volatile compounds. The data in Fig. 7 exhibit a slight inlet memory effect typified by a gradual rise in total HCN background signal over time after sampling gases from several cyanogenic plants. These effects can also be seen in the sloping rise of the HCN signal near sample maxima as well as gradual fall-off of the HCN mixing ratio after a sample is removed. This effect is less pronounced for acetone and butanone than for HCN and should not affect our results. The gradual contamination of the inlet by HCN might be eliminated by heating the inlet or by use of a shorter calibrated glass capillary for sample introduction. A slight background at $m/z$ 71 is observed while sampling humidified room air and is attributed to the adduct $OH^-(H_2O)_3$ anion. The average background contributes ~0.13 ppmv to the butanone signal at $m/z$ 71 and this value is uniformly subtracted from all subsequent quantification of butanone.

In order to ascertain that acetone and butanone are the precursor VOCs leading to signals at $m/z$ 57 and 71, H/D exchange data from standards were compared with $[M-1]^-$ anions generated by sampling headspace from the HCNpi variety of clover into the ion-source flow-tube. Fig. 6 summarizes the results of this experiment and gives the ratio of peak heights of $CD_3OD$-clustered product ions 94/93 and 108/107 observed following interaction of $m/z$ 57 with $CD_3OD$ and $m/z$ 71 with $CD_3OD$. Clustered product ions were compared since they had greater peak heights. Within experimental uncertainty, the ratios observed using a plant as the source of ions are closest to those observed when using pure acetone and butanone standards. This suggests that the identities of the compounds released by HCNpi clover are acetone and butanone rather than propanal or butanal. Following this measurement, pure aldehydes were also added to the plant gases and the observed ratios changed accordingly. The production of $[M-1]^-$ anions in the presence of water in the ion source raises the possibility of simultaneously SIFT injecting both the butanone $[M-1]^-$ anion at $m/z$ 71 and $OH^-(H_2O)_3$ anion, also at $m/z$ 71. However, no evidence exists that ion coincidence interfered with H/D exchange measurements. Based on these tests, if any aldehyde was present, it was below our detection limits. During separate experiments, sufficient densities of fragment ions could not be produced by SIFT–CID using a plant sample to use the data as a second, independent means of identification. Due to the well-documented occurrence and breakdown of cyanohydrin precursors, it is assumed that corresponding ions observed for other plants also belong to acetone and butanone exclusively.

The additional mass selection of a product that is already a minor component of the mass spectrum poses the largest obstacle in either SIFT–CID or H/D exchange experiments for confirming ion identities since

only very small ion concentrations are available for subsequent analysis. These experiments may be facilitated if performed in an instrument optimized for air-monitoring which is capable of producing higher product ion concentrations. Higher ion densities will allow effective use of $MS^n$ analyzers for identification or performance of subsequent ion/molecule reactions to probe ion structure.

In the leaves sampled here, high release of HCN was accompanied by high release of acetone and/or butanone in all cases. Those plants that did not produce observable amounts of HCN generated only small amounts of acetone and no detectable butanone. Release of HCN was fully expected for BLHplus clover, HCNpi clover, Aran clover [27,28], cassava [48], and eucalyptus [49] based on previous studies. However, the particular eucalyptus plants tested were shown separately to be acyanogenic clones that did not produce HCN. Results given in Fig. 7 show that the Dutch white clover was also acyanogenic. In separate experiments, seeds from a different bag of Dutch white clover showed significant cyanogenic character. Although it was impossible to predict whether seeds from an untested seed source would produce a cyanogenic plant, the relative amounts of HCN emission for a plant from a given seed source could be easily reproduced. It is interesting to note the extremely high emissions of HCN per gram of plant material observed for cassava in comparison to all other plants tested, especially in light of its use as a food staple in many countries.

If it is assumed that there are only two precursor compounds, linamarin and lotaustralin, giving rise to acetone, butanone, and HCN, then the sum of the acetone and butanone concentrations, prior to partitioning out of the plant, should be equal to the concentration of HCN. This balance has been verified in cyanogenic plants previously using membrane introduction mass spectrometry for acetone and butanone and a colorimetric assay for HCN [50]; unlike the work shown here, it was not possible to simultaneously analyze the ketone and HCN products of cyanogenic glycosides. Fig. 8 shows a plot of the HCN mixing ratio with respect to the sum of the acetone and butanone mixing ratios. The sum of these carbonyl compounds apparently falls significantly short of the concentration of HCN in the gas phase.

Henry's law, given in the following equation:

$$C_{aq} = k_H \times C_g \quad (6)$$

applies to dilute aqueous solutions although it can also be applied as a simple correction to account for differential partitioning of each species out of plant material. The variable $k_H$ is the dimensionless Henry's law constant, $C_g$ is the gas-phase concentration measured, and $C_{aq}$ is the aqueous phase concentration

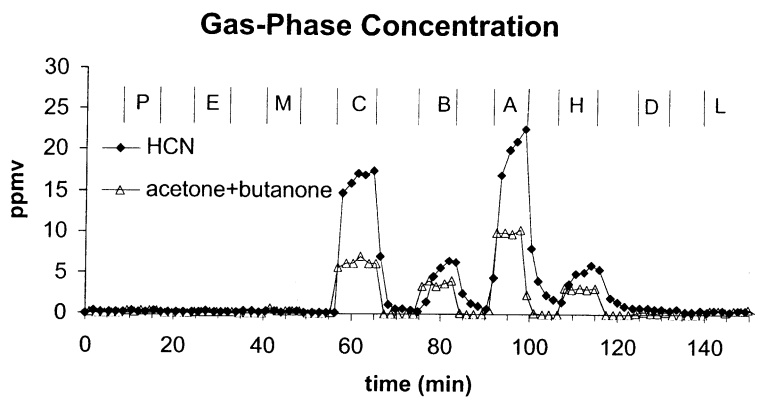


Fig. 8. Mixing ratio of HCN compared to the sum of acetone and butanone observed in sample headspace for nine different plants. Plants tested are described in more detail in Fig. 7, and include acyanogenic species (P, E, M, D, and L) and cyanogenic species (C, B, A, and H).

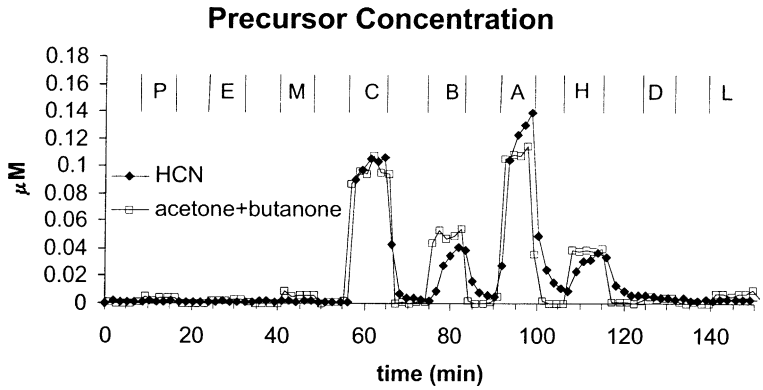


Fig. 9. Predicted concentration of the sum of linamarin and lotaustralin precursors from nine different plants using Henry's law and measured gas-phase concentrations. Plants tested are described in more detail in Fig. 7, and include acyanogenic species (P, E, M, D, and L) and cyanogenic species (C, B, A, and H).

or, in this case, the concentration of the precursor from which acetone, butanone and HCN are derived. Dimensionless Henry's law constants were obtained by multiplying average values obtained from Sander [51] by RT. The resulting values for $k_H$ are approximately 238 for HCN, 608 for acetone, and 356 for butanone. The value of $C_{aq}$ was then calculated for each data point using the $k_H$ values. The results of this calculation are shown in Fig. 9.

Even with such a simple model, a substantially improved balance between acetone, butanone, and HCN is obtained. The sum of acetone and butanone concentrations is seemingly higher than that of HCN for HCNpi and BLHplus clovers due to uncertainty in quantification, rather than from a second pathway for production of these compounds. This claim seems justified in light of the fact that the sum of acetone and butanone is lower than the concentration of HCN for Aran clover in which similar mechanisms should operate. These results suggest that breakdown of cyanogenic glycosides is the major pathway for production of these compounds.

Assuming any secondary release of carbonyls to be negligible in comparison to cyanogenesis and assuming complete or at least equivalent decomposition of any cyanogenic precursors present in the plant material, an estimate of the relative amounts of the lotaustralin and linamarin precursors can be easily obtained. For example, the cyanogenic varieties of clover examined here have the following ratios: Aran, 0.62; HCNpi, 1.26; and BLHplus, 2.75. These values can be compared to published linamarin/lotaustralin ratios for seven clover varieties, which ranged from 0.4 to 0.8 [52]. The higher ratios seen here could reflect a higher recovery of linamarin products, since the direct NI-CIMS analysis avoids the drying, extraction and HPLC procedure typically used in cyanogenic glycoside analysis [53]. Further testing, in which cyanogenic precursors are extracted and quantified in conjunction with the gas-phase measurement given here, is needed to verify that such an estimate is valid. If these estimates are reliable, the CIMS technique has advantages over current techniques [54] for large scale screening of plants for cyanogenesis and possibly for identification of specific cyanogenic precursors.

This type of measurement may provide information on carbonyls released by other cyanogenic precursors that have been reported in the literature. The Henry's law constant for benzaldehyde ($k_H \sim 950$) suggests that both breakdown products of prunasin (i.e., benzaldehyde and HCN) might be detectable in the same way as linamarin and lotaustralin. On the other hand, cyanogenic glycosides that might release hydroxy-benzaldehyde compounds (dhurrin, taxiphyllin, zierin, etc., $k_H \sim 10^7$), ketene (acacipetalin, $k_H$ unknown), and cyclopentenone compounds

(deidaclin, tetraphyllin B, gynocardin, $k_H$ unknown) may not be detectable in the gas-phase except through their HCN release.

## 4. Conclusions

The $OH^-$ anion is a useful chemical ionization reagent for on-line VOC monitoring with flow-reactor mass spectrometers. The $OH^-$ anion reacts with a wide variety of VOCs at collisional rates and affords simple reaction products, the possibility of fragment ion analysis, as well as the possibility of H/D exchange analysis for distinguishing isomeric anions. Many of the products of reaction between biogenic VOCs and $OH^-$ as well as $[M-1]^-$ ion fragments can be understood in light of previous work including various neutral loss products. Fragment ion and H/D exchange data show, once again, the utility of these techniques for identification of VOC precursors and their anionic products. Use of this species has aided in identification of HCN, acetone, and butanone released from wounded leaves and should provide other opportunities for analyzing and understanding complex mixtures of VOCs in the gas-phase.

Negative-ion chemical ionization and flow-reactor mass spectrometers in general have definite promise as screening tools for detecting the presence of cyanogenic glycosides in various plants. The exact quantities of these precursors should be examined by other methods in order to validate the results presented here. Further studies of plants containing cyanogenic glycosides are needed to determine whether this technique will work equally well for the wider variety of cyanogenic precursors that have been identified to date.

## Acknowledgements

We gratefully acknowledge support of this research by the National Science Foundation (CHE-0100664 and ATM-9805191) and by the CIRES Innovative Research Program. We thank Charles DePuy and Abigale Curtis for helpful discussions, Charles Grayless for plant maintenance, and Gary Pederson for providing clover seed.

## References

[1] A.G. Harrison, Chemical Ionization Mass Spectrometry, 2nd ed., CRC Press, Boca Raton, FL, 1982.
[2] H. Budzikiewicz, Mass Spectrom. Rev. 5 (1986) 345.
[3] B. Munson, Int. J. Mass Spectrom. 200 (2000) 243.
[4] S.T. Graul, R.R. Squires, Mass Spectrom. Rev. 7 (1988) 263.
[5] W. Lindinger, A. Hansel, A. Jordan, Int. J. Mass Spectrom. Ion Process. 173 (1998) 191.
[6] D. Smith, P. Spanel, Int. Rev. Phys. Chem. 15 (1996) 231.
[7] J.A. de Gouw, C.J. Howard, T.G. Custer, B.M. Baker, R. Fall, Environ. Sci. Technol. 34 (2000) 2640.
[8] R. Fall, T. Karl, A. Jordan, W. Lindinger, Atmos. Environ. 35 (2001) 3905.
[9] T. Reiner, O. Mohler, F. Arnold, J. Geophys. Res. 103 (1998) 31309.
[10] A. Hatanaka, Phytochemistry 34 (1993) 1201.
[11] E.E. Conn, Planta Med. 57 (1991) S1.
[12] E.P.L. Hunter, S.G. Lias, J. Phys. Chem. Ref. Data 27 (1998) 413.
[13] D.R. Lide, Jr., Gas-Phase Ion and Neutral Thermochemistry, American Chemical Society, Washington, DC, 1988.
[14] J.E. Bartmess, Mass Spectrom. Rev. 8 (1989) 297.
[15] K.R. Jennings, Int. J. Mass Spectrom. 200 (2000) 479.
[16] D.H. Russel (Ed.), Experimental Mass Spectrometry, Plenum Press, New York, 1994.
[17] N. Nibbering, Adv. Phys. Org. Chem. 24 (1988) 1.
[18] D.F. Hunt, S.K. Sethi, J. Am. Chem. Soc. 102 (1980) 6953.
[19] S. Campbell, M.T. Rodgers, E.M. Marzluff, J.L. Beauchamp, J. Am. Chem. Soc. 117 (1995) 12840.
[20] P. Spanel, M. Pavlik, D. Smith, Int. J. Mass Spectrom. Ion Process. 145 (1995) 177.
[21] J.M. Van Doren, S.E. Barlow, C.H. DePuy, V.M. Bierbaum, Int. J. Mass Spectrom. Ion Process. 81 (1987) 85.
[22] S. Kato, R. Gareyev, C.H. DePuy, V.M. Bierbaum, J. Am. Chem. Soc. 120 (1998) 5033.
[23] J.M. Van Doren, Ph.D. thesis, University of Colorado at Boulder, 1987.
[24] C.H. DePuy, V.M. Bierbaum, G.K. King, R.H. Shapiro, J. Am. Chem. Soc. 100 (1978) 2921.
[25] R.R. Squires, V.M. Bierbaum, J.J. Grabowski, C.H. DePuy, J. Am. Chem. Soc. 105 (1983) 5185.
[26] X. Lee, J. Geophys. Res. 105 (2000) 17807.
[27] G.A. Pederson, G.E. Brink, Agron. J. 90 (1998) 208.
[28] F. Saucy, J. Studer, V. Aerni, B. Schneiter, J. Chem. Ecol. 25 (1999) 1441.
[29] T. Su, W.J. Chesnavich, J. Chem. Phys. 76 (1982) 5183.
[30] Y. Ikezoe, S. Matsuoka, M. Takebe, A. Viggiano, Gas Phase Ion–Molecule Reaction Rate Constants through 1986, Maruzen Co. Ltd., Tokyo, Japan, 1987.
[31] G.I. Mackay, S.D. Tanner, A.C. Hopkinson, D.K. Bohme, Can. J. Chem. 57 (1979) 1518.

[32] A.B. Raksit, D.K. Bohme, Can. J. Chem. 61 (1983) 1683.
[33] S.D. Tanner, G.I. Mackay, D.K. Bohme, Can. J. Chem. 59 (1981) 1615.
[34] P. Spanel, D. Smith, Int. J. Mass Spectrom. Ion Process. 167–168 (1997) 375.
[35] D.R. Lide (Ed.), CRC Handbook of Chemistry and Physics, 81st ed., CRC Press, Boca Raton, FL, Copyright 2000.
[36] K.J. Miller, J.A. Savchik, J. Am. Chem. Soc. 101 (1979) 7206.
[37] J.C. Sheldon, J.H. Bowie, S. Dua, J.D. Smith, R.A.J. O'Hair, J. Org. Chem. 62 (1997) 3931.
[38] G.W. Haas, M.L. Gross, J. Am. Soc. Mass Spectrom. 7 (1996) 82.
[39] T.G. Custer, S. Kato, R. Fall, V.M. Bierbaum, Geophys. Res. Lett. 27 (2000) 3849.
[40] C.H. DePuy, V.M. Bierbaum, R. Damrauer, J.A. Soderquist, J. Am. Chem. Soc. 107 (1985) 3385.
[41] C.F. Bernasconi, M.W. Stronach, C.H. DePuy, S. Gronert, J. Phys. Org. Chem. 3 (1990) 346.
[42] G. Klass, J.C. Sheldon, J.H. Bowie, J. Chem. Soc., Perkin Trans. II 9 (1983) 1337.
[43] A.A. Viggiano, S.T. Arnold, R.A. Morris, Int. Rev. Phys. Chem. 17 (1998) 147.
[44] X. Yang, A.W. Castleman Jr., J. Am. Chem. Soc. 113 (1991) 6766.
[45] S.T. Arnold, A.A. Viggiano, J. Phys. Chem. A 101 (1997) 2859.
[46] P. Spanel, D. Smith, J. Phys. Chem. 99 (1995) 15551.
[47] P. Spanel, D. Smith, J. Am. Soc. Mass Spectrom. 12 (2001) 863.
[48] J.M. McMahon, W.L.B. White, R.T. Sayre, J. Exp. Bot. 46 (1995) 731.
[49] R.M. Gleadow, I.E. Woodrow, Aust. J. Plant Physiol. 27 (2000) 693.
[50] L.A.B. Moraes, M.N. Eberlin, J.R. Cagnon, L.H. Urbano, Analyst 125 (2000) 1529.
[51] R. Sander, Compilation of Henry's Law Constants for Inorganic and Organic Species of Potential Importance in Environmental Chemistry (Version 3), http://www.mpch-mainz.mpg.de/~sander/res/henry.html, 1999.
[52] A. Stochmal, W. Oleszek, J. Agric. Food Chem. 45 (1997) 4333.
[53] A. Stochmal, W. Oleszek, Phytochem. Anal. 5 (1994) 271.
[54] M.E. Alonso-Amelot, A. Oliveros, Phytochem. Anal. 11 (2000) 309.